

Article

Modulating Directional Movement of Graphene Nanoflake Using a Channel

Rui Li ^{1,*} , Ben An ¹, Jiahao Liu ¹ and Qing Peng ^{2,3,4,*} ¹ School of Mechanical Engineering, University of Science and Technology Beijing, Beijing 100083, China² Physics Department, King Fahd University of Petroleum and Minerals, Dhahran 31261, Saudi Arabia³ K.A.CARE Energy Research & Innovation Center at Dhahran, Dhahran 31261, Saudi Arabia⁴ Interdisciplinary Research Center for Hydrogen and Energy Storage, King Fahd University of Petroleum and Minerals, Dhahran 31261, Saudi Arabia

* Correspondence: lirui@ustb.edu.cn (R.L.); qing.peng@kfupm.edu.sa (Q.P.)

Abstract: The graphene-based nano-mechanical systems have attracted a lot of attention due to their unique properties. Owing to its planar shape, it is hard to control the direction of motion of graphene. In this study, a directional system based on graphene with a channel driven by a thermal gradient was examined by means of molecular dynamics simulations. The results showed that the channel could direct the motion and correct the rotation of graphene nanoflakes. The movement of graphene nanoflake not only depended on the interaction between the nanoflake and the substrate, but also the configuration of the graphene in the channel. A larger thermal gradient was needed to drive a hydrogen-passivated graphene nanoflake. However, the movement of a passivated nanoflake was more stable. Our results showed that a passivated graphene nanoflake could move steadily along a direction in a channel, which might shed light on the design of nano-mechanical systems based on graphene.

Keywords: graphene; motion; thermal gradient; channel; molecular dynamics



Citation: Li, R.; An, B.; Liu, J.; Peng, Q. Modulating Directional Movement of Graphene Nanoflake Using a Channel. *Crystals* **2022**, *12*, 1830. <https://doi.org/10.3390/cryst12121830>

Academic Editor: Igor Neri

Received: 25 November 2022

Accepted: 10 December 2022

Published: 15 December 2022

Publisher's Note: MDPI stays neutral with regard to jurisdictional claims in published maps and institutional affiliations.



Copyright: © 2022 by the authors. Licensee MDPI, Basel, Switzerland. This article is an open access article distributed under the terms and conditions of the Creative Commons Attribution (CC BY) license (<https://creativecommons.org/licenses/by/4.0/>).

1. Introduction

With the development of nano-mechanical and micro-mechanical systems, the movements of nanomaterials in designed systems have attracted extensive attention. Many kinds of methods have been applied to control the movements of nanomaterials, such as atom force measurement (AFM) [1,2], electronic field [3–6], magnetic field [7], stiffness gradient [8,9], strain field [10,11], friction between interfaces [12–14], surface dynamics [15], and thermal energy [16–19]. Among them, the thermal gradient method has been one of the most important, owing to the ease of operability.

Carbon nanomaterials play an important role in nano-mechanical systems. Naturally, quite a few researchers have accomplished significant work on driving carbon nanomaterials by thermal gradients. The tubular shape of a carbon nanotube makes it an excellent candidate for use in nano-mechanical systems. Barreiro et al. [20] investigated the subnanometer motion of cargo driven by thermal gradients along carbon nanotubes. Rurail et al. [21] studied the directed motion of fullerene clusters inside carbon nanotubes by a thermal gradient. Hou et al. [22] investigated the actuation induced by a thermal gradient in a double-walled carbon nanotube. Shenai et al. [23,24] also conducted similar research on a double-walled carbon nanotube. Guo et al. [25] investigated the mechanics of a double-walled carbon nanotube device driven by a thermal gradient. Santamaría-Holek et al. [26] presented a model to describe the dynamics of a double-walled carbon nanotube motor driven by a thermal gradient. Oyarzua et al. [27] designed a thermally induced water pump based on a carbon nanotube. Lin et al. [28] investigated the self-thermophoretic motion of controlled assembled micro-/nanomotors. Zhu et al. [29] studied the continuous cyclic motion of a system based on carbon nanotubes driven by a stable thermal field. Graphene has also attracted a great deal of attention, owing to its excellent

thermal and mechanical properties. Lohrasebi et al. [30] investigated the motion of C_{60} on a graphene sheet driven by a temperature gradient. Chen et al. [31] studied the process of water transport in a graphene channel for water desalination. Becton et al. [32] indicated that a thermal gradient could drive graphene flake to move on a substrate.

Although significant work has been conducted on the systems based on graphene driven by thermal gradients, researchers have found that the motion of the graphene is relatively hard to control. The reason is related to the shape of a graphene sheet. Unlike carbon nanotubes, which have a tubular shape that can direct the motion along the tube, the planar shape of graphene results in rotation; thus, it is hard to control its motion. Therefore, in this paper, we have investigated the effect of a graphene channel on the motion of a graphene nanoflake on a substrate at a thermal gradient. The results showed that the channel could direct the motion and correct the rotation of the graphene nanoflake. Our results might shed light on the construction of nano-mechanical systems based on graphene.

2. Model and Method

Becton et al. [32] indicated that the shapes of a square and a circle had smaller linear velocity and larger angular velocity, owing to more rotationally symmetrical edges, which implied that it was more difficult to control their motion. Therefore, in this study, the models were composed of a square graphene nanoflake with a width of 2.0 nm and a graphene substrate. Two kinds of models were examined for comparison: models with and without a graphene channel, as shown in Figure 1a,b, respectively. They are hereafter denoted as the graphene channel model and normal model, respectively. For each model, the graphene nanoflake was pristine or hydrogen-passivated, as shown in Figure 1c. Notably, the outer free electrons of C atoms were all saturated. It was an ideal condition, one that involved more hydrogen atoms than in the experiments; however, this did not obviously influence the results. The substrate included two graphene layers. The layer size was 10.1 nm and 20.0 nm along the x and y directions, respectively. All of the atoms of the lower layer of the substrate were fixed to mimic the bulk phase of the substrate. The upper layer of substrate was fixed on both ends to model the surface. For the channel model, as shown in Figure 1b,e, the channel was composed of two smaller graphene sheets, in which the inner side of the graphene was grafted with hydrogen atoms to passivate the dangling bonds. The width of the channel was 4.1 nm. The periodic conditions were applied along the x and y directions.

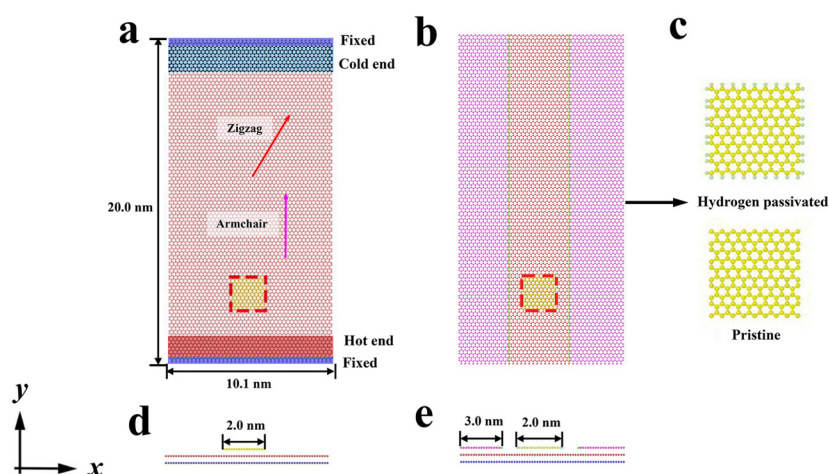


Figure 1. The setup of models. The vertical (a) and side (d) views of the model without channel; (b,e) were the vertical and front views of the model with graphene channel. The brown and blue balls denoted graphene substrates. The purple balls denoted the graphene sheet that forms the channel. The green–yellow atoms were hydrogen atoms and carbon atoms of graphene nanoflake. (c) The pristine and hydrogen-passivated graphene nanoflakes.

The potential of AIREBO [33] was successfully applied to describe the bond interaction among C and H atoms, especially for carbon nanomaterials; therefore, it was applied to describe the interaction among C and H atoms in the graphene sheet. The 12-6 L-J potential [34] was used for the van der Waals interaction between the C and C, and the C and H, atoms. The time step was 0.001 ps. First, the canonical ensemble (NVT ensemble) was applied for 20 ps with a system temperature of 300 K controlled by the Langevin thermostat method to make the system reach equilibrium. Then, the hot and cold ends were set on the substrate. The temperatures of the hot and cold ends were 600 K and 300 K, respectively; and the NVT ensemble was then applied to the two zones to maintain the thermal gradient in the system, as shown in Figure 1a. The microcanonical ensemble (NVE ensemble) was applied for carbon atoms in the middle of the graphene substrate. Then, heat flowed from the hot end to the cold end, and the whole system reached equilibrium after a period of time. All of the simulations were carried out using Large-Scale Atomic/Molecular Massively Parallel Simulator (LAMMPS) [35].

Coluci et al. [36] noted that the thermal gradient was not constant, owing to the heat conduction when the hot and cold ends were initially set. For this work, the potential of the whole system reached equilibrium at 60 ps, which meant that the thermal gradient became stable after 60 ps. Therefore, the centroid of the graphene nanoflake was fixed during this period (60 ps). After the stabilization of the thermal gradient, the graphene nanoflake was released. Then, the thermal gradient drove the graphene nanoflake to move on the substrate.

3. Results and Discussion

3.1. The Effect of a Channel

The effect of a channel on the movement of a graphene nanoflake was investigated via the comparison between the two cases with and without the channel. When the stable thermal gradient was achieved, the graphene nanoflake was unfixed. The movement of the pristine graphene nanoflake along the x and y directions is shown in Figure 2 for models with and without the channel. The thermal gradient was 15 K/nm. The movement of the graphene nanoflakes along the y direction was similar for the two cases. They both reached the cold end of the substrate at about 80 ps. However, the movement along the x direction showed obvious difference in two cases. The graphene nanoflake moved along the whole channel in the channel model (20 nm). In contrast, it moved about 2.6 nm along the x direction in the normal model.

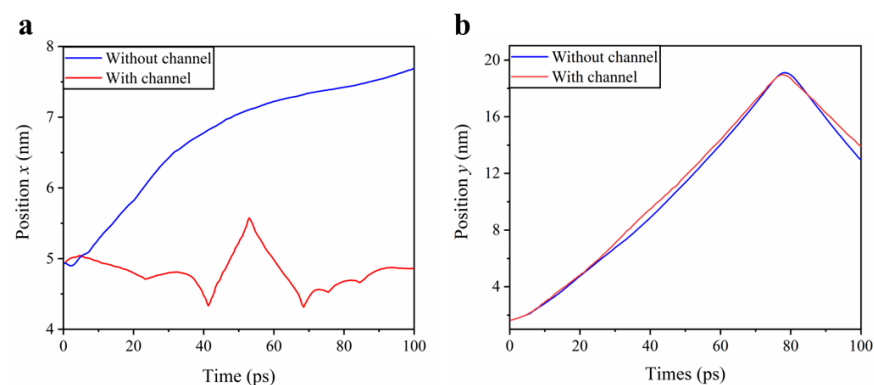


Figure 2. The evolution of the position of the centroid of graphene nanoflake. (a) Along x direction. (b) Along y direction.

To further observe the movement of the graphene nanoflake, snapshots were shown in Figures 3a–c and 3d–f for the normal model and the channel model, respectively. In Figure 3b,c, for the normal model, the graphene nanoflake drifted along in the y direction. It rotated gradually while moving along in the x direction. This observation was consistent with the reported results [20]. For the channel model, although the graphene nanoflake also

turned at an angle at the first stage, the channel could correct the rotation of the graphene nanoflake and guide the movement of the nanoflake. Then, the nanoflake moved in the channel along the y direction with two sides parallel to the channel. The correction of the rotation by the channel could be attributed to the interaction between the channel and the graphene nanoflake. The interaction is mainly governed by the van der Waals interaction, which can be approximated by a 12-6 Lennard-Jones potential: $U = 4\epsilon\left(\left(\frac{\sigma}{r}\right)^{12} - \left(\frac{\sigma}{r}\right)^6\right)$. The two banks of the channel interacted with the nanoflake, resulting in a potential well in the channel. The nanoflake was therefore stable in the central region of the channel. As shown in Figure 3e, the left side of the nanoflake was much closer to the edge of the channel than the right side, which resulted in an unbalanced larger van der Waals force on the nanoflake, according to the L-J potential. The imbalance of force on the two sides drove the nanoflake back to the center of the channel. Meanwhile, the force on the upper and lower sides of the nanoflake was also unbalanced when it turned at an angle, which rotated the nanoflake back to the configuration with the two sides parallel to the channel. Therefore, the graphene nanoribbon channel could correct the rotation of the graphene.

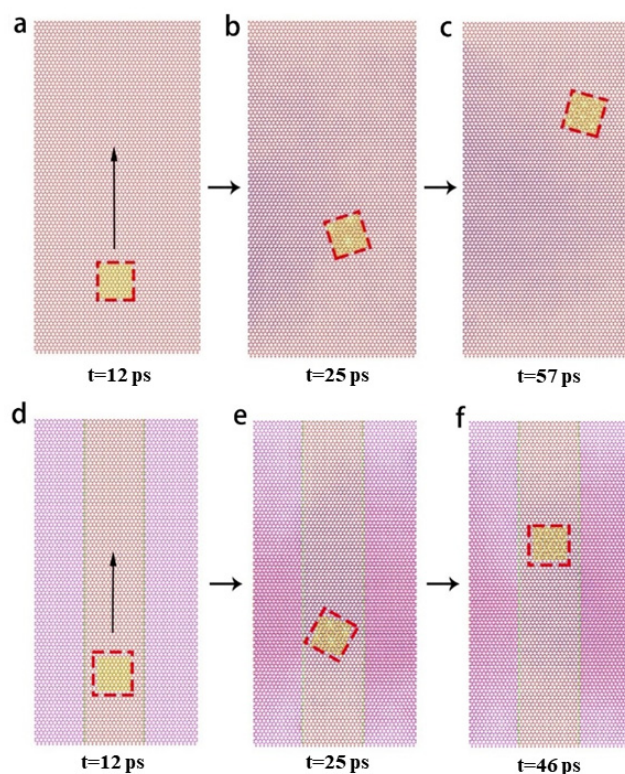


Figure 3. The snapshots of the movement of the nanoflakes. (a–c) Graphene nanoflake moved in the normal model. (d–f) Graphene nanoflake moved in the channel model.

3.2. The Effect of the Passivating Hydrogen Atoms

There are dangling bonds at the edge of pristine graphene nanoflakes, which may affect the movement of graphene. Figure 1c showed the passivation of a graphene nanoflake by hydrogen atoms. The movements of pristine and passivated graphene nanoflakes were shown in Figure 4. The thermal gradient was 10 K/nm. The passivated graphene nanoflake reached the cold end at about 1200 ps, so was faster than the pristine graphene. Moreover, oscillation occurred in the movement of the pristine graphene nanoflake, which moved back from $y = 1.8$ nm to $y = 1.2$ nm at about 1300–1500 ps, as shown in Figure 4a. Furthermore, the movement of the passivated graphene nanoflake along the x direction was also more stable, as shown in Figure 4b.

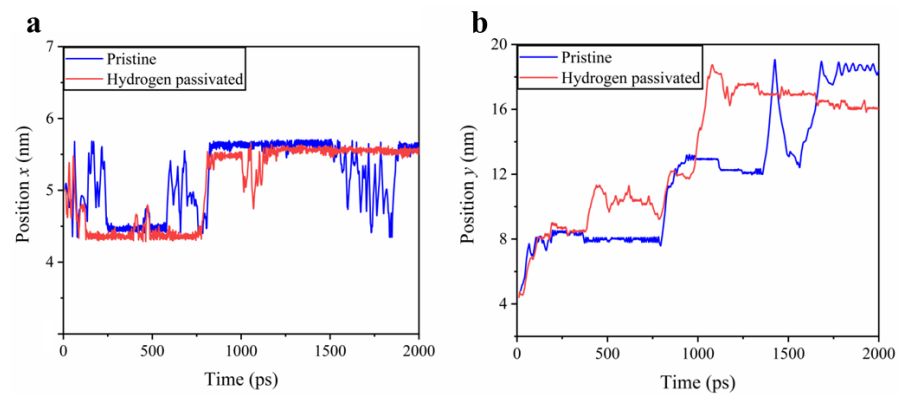


Figure 4. The movement of pristine and hydrogen-passivated graphene nanoflakes. (a) Along x direction. (b) Along y direction.

The binding energy between the passivated graphene nanoflake and the graphene substrate was 8.08 eV, which was 0.66 eV higher than that of the pristine graphene nanoflake and the substrate. The reason was that there were more atoms in the passivated nanoflake than in the pristine nanoflake. The stronger interaction seemed to form a deeper channel so that the thermophoresis movement was slower. However, the rotation of the nanoflakes in the channel also affected the movement. The snapshots of the two systems, with the pristine and the passivated graphene nanoflakes, were shown in Figures 5a–d and 5e,f, respectively. In Figure 5b,e,f, the rotation of the nanoflakes caused a small distance between them and the substrate, resulting in a stronger interaction than in the center of the channel, which slowed down the movement of the nanoflakes. The pristine and hydrogen-passivated graphene nanoflakes both turned at an angle at first. Although pristine and passivated graphene nanoflakes both returned to the configuration with two sides parallel to the channel in the cold end, the passivated nanoflake more quickly returned to the center of the channel. Combining the effects of the rotation and the interaction between the nanoflakes and the substrate, the passivated graphene nanoflake reached the cold end earlier.

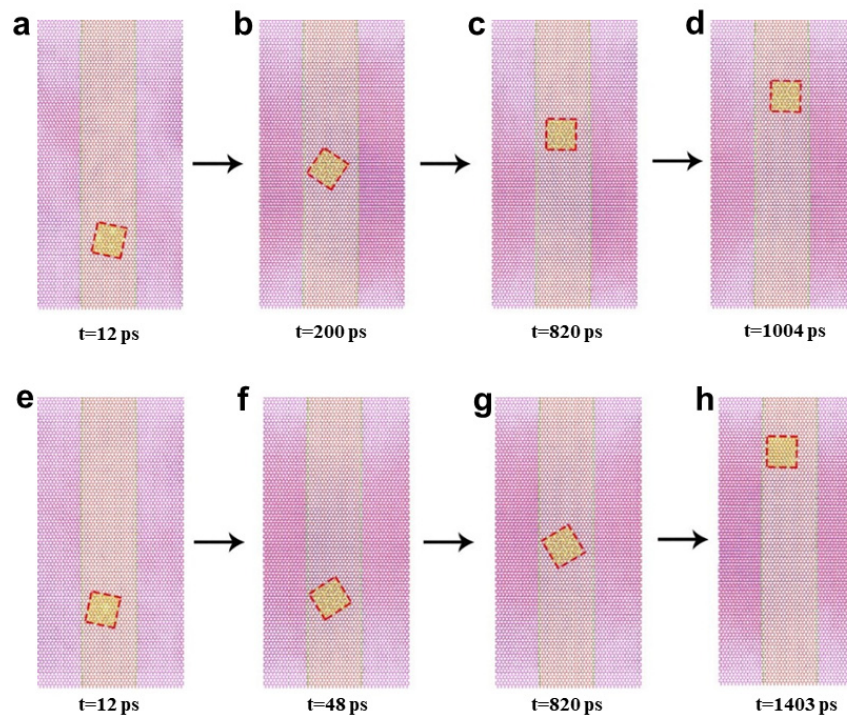


Figure 5. The snapshots of two systems during the movement. (a–d) Hydrogen-passivated graphene nanoflake. (e–h) Pristine graphene nanoflake.

3.3. The Effect of a Thermal Gradient

The thermal gradient drove the graphene nanoflake to move on the substrate. The magnitude of the thermal gradient appears to play an important role. The simulation results of the movements of pristine and hydrogen-passivated graphene nanoflakes under different thermal gradients were illustrated in Figure 6. For both pristine and passivated graphene systems, in this study, the larger thermal gradient led to faster movement of the nanoflakes when the thermal gradient was lower than 5 K/nm. The hydrogen-passivated graphene nanoflake could not move to the cold end successfully, as shown in Figure 6b. However, Figure 6a showed that the pristine graphene nanoflake reached the cold end. The reason could be attributed to the stronger interaction between the hydrogen-passivated graphene and the substrate, which formed an energy barrier that needed to be overcome by thermal energy. Then, a larger thermal gradient was needed to drive the passivated graphene nanoflake.

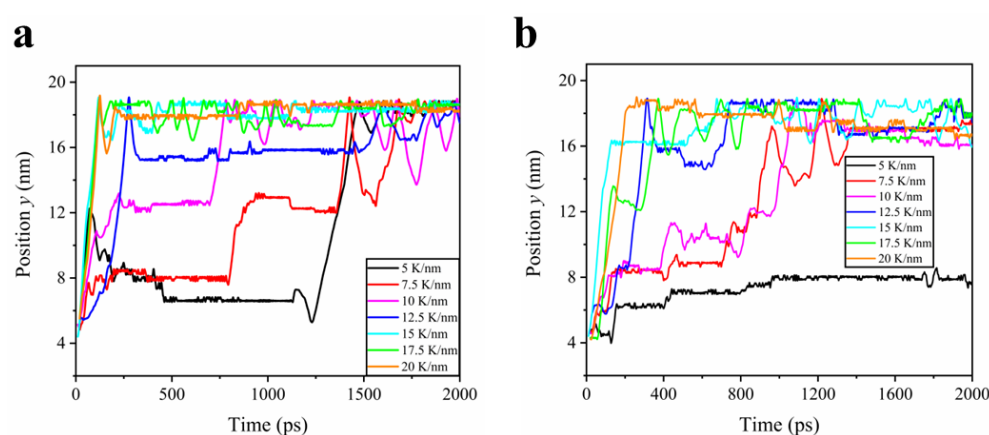


Figure 6. The movements of graphene nanoflakes along y direction for (a) pristine and (b) hydrogen-passivated graphene under various thermal gradients from 5 K/nm to 20 K/nm.

When the thermal gradient was larger than 12.5 K/nm, the response of the pristine graphene was slightly faster. The graphene nanoflakes moved to the cold end quickly at thermal gradients 17.5 and 20 K/nm. However, when the thermal gradient was 7.5 and 10 K/nm, the hydrogen-passivated graphene more quickly reached equilibrium in the cold end. The reason might be that the pristine graphene nanoflake kept the configuration with a turning angle for a longer time, as discussed in Section 3.2. The results imply that the movement of the passivated graphene square is more stable.

4. Conclusions

We investigated a graphene-based directional moving system driven by a thermal gradient by means of molecular dynamics simulations. The results showed that a graphene-nanoribbon-formed channel was capable of modulating the graphene nanoflake to move in a specific direction. Within the graphene channel, the graphene nanoflake turned at an angle at first, akin to how it moved outside the graphene channel. However, the graphene nanoflake returned to the center of the channel with two sides parallel to the channel edges, because the unbalanced force between it and the two edges of channel tended to rotate the nanoflake back. Our results showed that a channel consisting of graphene nanoribbon could effectively guide the motion of a graphene nanoflake.

The interaction between the passivated nanoflake and the graphene substrate was stronger than that of the pristine nanoflake. As a result, a larger thermal gradient was needed to drive a passivated graphene nanoflake. When the thermal gradient was lower than 5 K/nm, the passivated graphene could not be driven successfully. At a large thermal gradient, a passivated and pristine graphene nanoflake both quickly moved along the channel. The movement of the graphene not only depended on the interaction between the

graphene nanoflake and the substrate, but also the rotation of the graphene nanoflake in the channel. The rotation slowed down the movement. Oscillation sometimes occurred in the movement of pristine graphene nanoflake. The movement of passivated graphene was more stable. Our results might shed light on the design of nano-mechanical systems based on graphene.

Author Contributions: Conceptualization, R.L.; Methodology, B.A. and J.L.; Formal analysis, R.L., B.A., J.L. and Q.P.; Investigation, B.A. and J.L.; Writing—original draft, R.L. and B.A.; Writing—review & editing, Q.P. All authors have read and agreed to the published version of the manuscript.

Funding: The work was supported by the Fundamental Research Funds for the Central Universities (No. FRF-IDRY-20-008). Q.P. would like to acknowledge the support provided by the Deanship of Scientific Research (DSR) at King Fahd University of Petroleum and Minerals (KFUPM) for funding this work through project No. DF201020.

Data Availability Statement: The data presented in this study are available on request from the corresponding author.

Conflicts of Interest: The authors declare no conflict of interest.

References

1. Omidi, E.; Korayem, A.; Korayem, M. Sensitivity analysis of nanoparticles pushing manipulation by AFM in a robust controlled process. *Precis. Eng.* **2013**, *37*, 658–670. [[CrossRef](#)]
2. Feng, X.; Kwon, S.; Park, J.Y.; Salmeron, M. Superlubric sliding of graphene nanoflakes on graphene. *ACS Nano* **2013**, *7*, 1718–1724. [[CrossRef](#)] [[PubMed](#)]
3. Tu, Z.; Hu, X. Molecular motor constructed from a double-walled carbon nanotube driven by axially varying voltage. *Phys. Rev. B* **2005**, *72*, 033404. [[CrossRef](#)]
4. Wang, B.; Vuković, L.; Král, P. Nanoscale rotary motors driven by electron tunneling. *Phys. Rev. Lett.* **2008**, *101*, 186808. [[CrossRef](#)] [[PubMed](#)]
5. Kakade, M.V.; Givens, S.; Gardner, K.; Lee, K.H.; Chase, D.B.; Rabolt, J.F. Electric field induced orientation of polymer chains in macroscopically aligned electrospun polymer nanofibers. *J. Am. Chem. Soc.* **2007**, *129*, 2777–2782. [[CrossRef](#)]
6. Rahman, M.M.; Chowdhury, M.M.; Alam, M.K. Rotating-Electric-Field-Induced Carbon-Nanotube-Based Nanomotor in Water: A Molecular Dynamics Study. *Small* **2017**, *13*, 1603978. [[CrossRef](#)]
7. Lansdorp, B.M.; Tabrizi, S.J.; Dittmore, A.; Saleh, O.A. A high-speed magnetic tweezer beyond 10,000 frames per second. *Rev. Sci. Instrum.* **2013**, *84*, 044301. [[CrossRef](#)]
8. Theodorakis, P.E.; Egorov, S.A.; Milchev, A. Stiffness-guided motion of a droplet on a solid substrate. *J. Chem. Phys.* **2017**, *146*, 244705. [[CrossRef](#)]
9. Chen, S.; Cheng, Y.; Zhang, G.; Zhang, Y.-W. Spontaneous directional motion of water molecules in single-walled carbon nanotubes with a stiffness gradient. *Nanoscale Adv.* **2019**, *1*, 1175–1180. [[CrossRef](#)]
10. Khan, M.B.; Wang, S.; Wang, C.; Chen, S. Rotation of nanoflake driven by strain gradient fields in locally-indented graphene. *Nanotechnology* **2019**, *31*, 015303. [[CrossRef](#)]
11. Peng, Z.; An, H.; Yang, Y. The directional motion of nano-objects induced by an inhomogeneous strain field. *Acta Mech.* **2019**, *230*, 3295–3305. [[CrossRef](#)]
12. Cumings, J.; Zettl, A. Low-friction nanoscale linear bearing realized from multiwall carbon nanotubes. *Science* **2000**, *289*, 602–604. [[CrossRef](#)]
13. Zheng, Q.; Jiang, Q. Multiwalled carbon nanotubes as gigahertz oscillators. *Phys. Rev. Lett.* **2002**, *88*, 045503. [[CrossRef](#)]
14. Guo, W.; Guo, Y.; Gao, H.; Zheng, Q.; Zhong, W. Energy dissipation in gigahertz oscillators from multiwalled carbon nanotubes. *Phys. Rev. Lett.* **2003**, *91*, 125501. [[CrossRef](#)]
15. Xu, L.; Han, G.; Hu, J.; He, Y.; Pan, J.; Li, Y.; Xiang, J. Hydrophobic coating-and surface active solvent-mediated self-assembly of charged gold and silver nanoparticles at water–air and water–oil interfaces. *Phys. Chem. Chem. Phys.* **2009**, *11*, 6490–6497. [[CrossRef](#)]
16. Zambrano, H.A.; Walther, J.H.; Jaffe, R.L. Thermally driven molecular linear motors: A molecular dynamics study. *J. Chem. Phys.* **2009**, *131*, 241104. [[CrossRef](#)]
17. Cai, K.; Yu, J.; Shi, J.; Qin, Q.H. Spectrum of temperature-dependent rotational frequency of the rotor in a thermally driven rotary nanomotor. *J. Phys. Chem. C* **2017**, *121*, 16985–16995. [[CrossRef](#)]
18. Cai, K.; Wan, J.; Qin, Q.H.; Shi, J. Quantitative control of a rotary carbon nanotube motor under temperature stimulus. *Nanotechnology* **2016**, *27*, 055706. [[CrossRef](#)]
19. Piazza, R. Thermophoresis: Moving particles with thermal gradients. *Soft Matter* **2008**, *4*, 1740–1744. [[CrossRef](#)]
20. Barreiro, A.; Rurali, R.; Hernández, E.R.; Moser, J.; Pichler, T.; Forro, L.; Bachtold, A. Subnanometer motion of cargoes driven by thermal gradients along carbon nanotubes. *Science* **2008**, *320*, 775–778. [[CrossRef](#)]
21. Rurali, R.; Hernandez, E. Thermally induced directed motion of fullerene clusters encapsulated in carbon nanotubes. *Chem. Phys. Lett.* **2010**, *497*, 62–65. [[CrossRef](#)]

22. Hou, Q.-W.; Cao, B.-Y.; Guo, Z.-Y. Thermal gradient induced actuation in double-walled carbon nanotubes. *Nanotechnology* **2009**, *20*, 495503. [[CrossRef](#)] [[PubMed](#)]
23. Shenai, P.M.; Ye, J.; Zhao, Y. Sustained smooth dynamics in short-sleeved nanobearings based on double-walled carbon nanotubes. *Nanotechnology* **2010**, *21*, 495303. [[CrossRef](#)]
24. Shenai, P.M.; Xu, Z.; Zhao, Y. Thermal-gradient-induced interaction energy ramp and actuation of relative axial motion in short-sleeved double-walled carbon nanotubes. *Nanotechnology* **2011**, *22*, 485702. [[CrossRef](#)] [[PubMed](#)]
25. Guo, Z.; Chang, T.; Guo, X.; Gao, H. Mechanics of thermophoretic and thermally induced edge forces in carbon nanotube nanodevices. *J. Mech. Phys. Solids* **2012**, *60*, 1676–1687. [[CrossRef](#)]
26. Santamaría-Holek, I.; Reguera, D.; Rubi, J. Carbon-nanotube-based motor driven by a thermal gradient. *J. Phys. Chem. C* **2013**, *117*, 3109–3113. [[CrossRef](#)]
27. Oyarzua, E.; Walther, J.H.; Megaridis, C.M.; Koumoutsakos, P.; Zambrano, H.A. Carbon nanotubes as thermally induced water pumps. *ACS Nano* **2017**, *11*, 9997–10002. [[CrossRef](#)]
28. Lin, X.; Si, T.; Wu, Z.; He, Q. Self-thermophoretic motion of controlled assembled micro-/nanomotors. *Phys. Chem. Chem. Phys.* **2017**, *19*, 23606–23613. [[CrossRef](#)]
29. Zhu, F.; Guo, Z.; Chang, T. Nanoscale continuous cyclic motion driven by a stable thermal field. *Appl. Mater. Today* **2020**, *18*, 100520. [[CrossRef](#)]
30. Lohrasebi, A.; Neek-Amal, M.; Ejtehadi, M. Directed motion of C 60 on a graphene sheet subjected to a temperature gradient. *Phys. Rev. E* **2011**, *83*, 042601. [[CrossRef](#)]
31. Chen, B.; Jiang, H.; Liu, H.; Liu, K.; Liu, X.; Hu, X. Thermal-driven flow inside graphene channels for water desalination. *2D Mater.* **2019**, *6*, 035018. [[CrossRef](#)]
32. Becton, M.; Wang, X. Thermal gradients on graphene to drive nanoflake motion. *J. Chem. Theory Comput.* **2014**, *10*, 722–730. [[CrossRef](#)]
33. Stuart, S.J.; Tutein, A.B.; Harrison, J.A. A reactive potential for hydrocarbons with intermolecular interactions. *J. Chem. Phys.* **2000**, *112*, 6472–6486. [[CrossRef](#)]
34. Ruoff, R.; Hickman, A. Van der Waals binding to fullerenes to a graphite plane. *J. Phys. Chem.* **1993**, *97*, 2494–2496. [[CrossRef](#)]
35. Plimpton, S. Fast parallel algorithms for short-range molecular dynamics. *J. Comput. Phys.* **1995**, *117*, 1–19. [[CrossRef](#)]
36. Coluci, V.; Timoteo, V.; Galvao, D. Thermophoretically driven carbon nanotube oscillators. *Appl. Phys. Lett.* **2009**, *95*, 253103. [[CrossRef](#)]